JAPANESE JOURNAL OF APPLIED PHYSICS
Vol.47, No.1 (2008) pp.11-18 : Invited Review Paper

Development of Electron Holography and Its Applications to Fundamental Problems in Physics

Akira Tonomura[1,2,3,*]

We can now utilize the wave properties of electrons to conduct fundamental experiments on quantum mechanics because of the development of brighter electron beams as well as the ability directly to image the quantum world by utilizing the phase information of electrons. In this paper, we describe new possibilities that have been generated by electron-phase microscopy using electron microscopes equipped with coherent yet bright electron beams.

KEYWORDS: electron holography, Lorentz microscopy, superconductor, vortex, ferromagnet, Nb, YBCO, Bi-2212

1. Introduction

Electron holography was devised by Gabor almost six decades ago as a means of breaking through the resolution limit of electron microscopes.[1)] He invented a two-step imaging method, holography, to break through the resolution limit caused by the absence of aberration-free lens systems in electron microscopy. In holography, a hologram is first formed with electrons as an interference pattern between the object wave and a reference wave. The hologram is then illuminated by a reference optical wave to reconstruct the electron wavefronts as optical wavefronts.

In electron holography, the aberrations in the electron lens system can be optically compensated for in its reconstruction stage. Gabor's original approach was in-line holography, where the electron wave passing around the object is used as a reference wave.[1)] This kind of hologram is, so to speak, a defocused electron micrograph photographed under coherent illumination, similar to the Fresnel fringes first reported by Boersch.[2)]

Although the idea of holography was first demonstrated in optical experiments by Gabor,[1)] the first experiment on electron holography was carried out by Haine and Mulvey,[3)] using the in-line method. Their reconstructed image was, however, disturbed by the Fresnel fringes that are produced by the conjugate image, which is always formed in addition to the reconstructed image in holography. Hibi[4)] obtained similar results using a pointed filament he developed as a coherent electron source.

The reconstruction of clear images, free from the effects of conjugate images, was first demonstrated by Leith and Upatnieks[5)] using off-axis laser holography, where the reconstructed and conjugate images could be separated into two beams traveling in different directions. It was also demonstrated optically by DeVelis *et al*.[6)] that image reconstruction free of conjugate-image disturbances is possible even in an in-line holography provided that holograms are formed in the Fraunhofer diffraction area of the object.

Encouraged by this experiment, Tonomura *et al*.[7)] demonstrated an electron version of this Fraunhofer holography using a 100 kV electron microscope equipped with a pointed cathode, and clear-cut images were first obtained. This in-line holography entailed some limitations, such as small sizes for objects surrounded by clear spaces. However, the coherence conditions required for the illuminating electron beam are much less stringent than those for off-axis holography.

Off-axis electron holography was first carried out by Möllenstedt and Wahl,[8)] which however had to be made in one-dimensional imaging to make up for the poor coherence of the electron beam. A slit-shaped electron source was employed to form a hologram with many carrier fringes, and an image of a one-dimensional tungsten filament was optically reconstructed.

Image formation using electron holography was thus confirmed to be feasible. The resolution of the reconstructed images was low (~50 Å) and no new information was obtained by the holography. The practical realization of electron holography had to wait for the development of a coherent field-emission electron source, just as optical holography had to wait for the invention of lasers.

In this paper, we provide an overview of the present status of electron holography, with special reference to its recent applications to problems on fundamental physics and also on technological frontiers.

2. Developments in Holography due to Advent of Coherent Beams

We describe the historical development of electron holography here with advances in coherent beam technology, since a bright electron source using field emissions was the most decisive factor in the development of electron holography.

Although field emissions were already used in a field-emission microscope to observe the tip surface with atomic-scale resolution early in the 20th century,[9)] it was Crewe *et al*.[10)] who developed a practical field-emission gun for the scanning electron microscope (SEM) or scanning transmission electron microscope (STEM), and greatly improved their resolutions, particularly that of STEM, reaching down to atomic dimensions.[11)] This beam is also suitable as a coherent beam for electron interferometery; its brightness is greater than that of a thermionic beam by more than three orders of magnitude, mainly because a strong electric field on the surface of the cathode tip produces no space-charge effect. In addition, the energy spread of the beam is as narrow as 0.3 eV when the emission current is limited to 10 μA. This source was first used only for scanning microscopes, and its acceleration voltage was limited to 30 kV.

1 Advanced Research Laboratory, Hitachi, Ltd., Hatoyama, Saitama 350-0395, Japan
2 Frontier Research System, RIKEN, Wako, Saitama 351-0198, Japan
3 Okinawa Institute of Science and Technology, Kunigami, Okinawa 904-0411, Japan
* E-mail address: akira.tonomura.zk@hitachi.com
(Received May 28, 2007; accepted September 7, 2007; published online January 18, 2008)

We started the development of a field-emission electron beam at Hitachi in 1967 soon after our experiments on in-line Fraunhofer electron holography.[7] From our experience with the holography experiments, we realized that bright electron beams, e.g., laser beams, would be needed to apply such holographic techniques to high-resolution microscopy for practical use. In fact, the resolution of the reconstructed images using a pointed filament[4] in our early experiments[7] did not even reach that of conventional electron microscopes due to the poor coherence of electron beam. Our original objective to overcome the resolution limit of the electron microscopes by compensating for the aberrations in electron lenses was by no means achieved.

We began to develop brighter field-emission electron beams in 1967 and we have continued the effort up to now. Accelerated electron-beam voltages higher than 50 kV are needed for transmission electron microscopes. However, this development was not easy, since the electric discharge of the high voltage in the electron gun easily destroyed the tip. In addition, since the extremely small electron source, typically 50 Å in diameter, had to be immobilized to within a fraction of the source diameter, we had to prevent even the slightest mechanical vibration of the tip, the accelerating tube, or microscope column, or the deflection of the fine beam by stray ac magnetic fields. Otherwise, the inherent brightness or luminosity of the electron beam would deteriorate.

After ten years of work, we developed an 80 kV electron beam,[12] which was two orders of magnitude brighter than that of the thermal beams used then (see Table I). Using the beam, we were able to observe electron interference patterns directly on a fluorescent screen for the first time, and we were able to take as many as 3000 interference fringes on a film, whereas 300 fringes had been the maximum up to that time. New information that had been inaccessible with conventional electron microscopy can now be obtained by using electron holography. Since the first successful development of a bright field-emission electron beam in 1979, we have continued to develop even brighter electron beams. This was mainly achieved by increasing the beams' accelerating voltages. An electron gun with a higher energy is larger and has thus more space to introduce additional electron-optical systems to minimize the blurring of the image of the tiny electron source due to aberrations during the acceleration process, e.g., by adding a magnetic lens to the electron gun.

Every time we increased brightness, new possibilities opened up as shown in Table I. Specific examples can be found in the magnetic lines of force in the microscopic region, which were directly and quantitatively observed in h/e flux units[13] in an interference micrograph with an 80 kV microscope. We were able to measure the phase shifts with a precision as small as 1/100 of an electron wavelength with a 250 kV microscope,[14] and carried out experiments on the Aharonov–Bohm (AB) effect. We observed the real time dynamics of vortices in metal[15] and high-T_c superconductors[16] with 350 kV[17] and 1 MV microscopes.[18] In general, the brightness of an electron beam is proportional to the accelerating voltage. In reality, however, the brightness of the electron beam obtained at 1 MV is 2×10^{10} A/(cm$^2 \cdot$ster), which is more than one order of magnitude higher than the expected value (1.2×10^9) estimated from the brightness at 80 kV. This is due to the decrease in the aberrations realized by introducing a magnetic lens to the accelerating region. The maximum number of biprism interference fringes with this beam increased from 3,000 to 11,000.[19]

We settled the controversy about the existence of the AB effect (see § 3.2.2) in 1986 through a series of experiments[20–22] using electron holography without ambiguities about leakage magnetic fluxes from solenoids or magnets.

3. Applications

3.1 High-resolution microscopy

The resolution of the reconstructed images has been greatly improved due to the advent of the field-emission electron beams. For example, Munch[23] used a field-emission beam to improve the resolution up to 10 Å using the in-line Fraunhofer holography.

Lattice images with 2.4 Å spacing were reconstructed by Tonomura *et al.*[24] using off-axis holography, and spherical aberrations of the reconstructed images were compensated for using the corresponding optical convex lens in the optical reconstruction stage.[25] Lichte[26] numerically reconstructed the lattice fringes of carbon black using hologram carrier fringes (0.8 Å) narrower than lattice fringes. The reconstructed-image resolution was further improved and the aberrations were corrected by Orchowski *et al.*[27] Further progress was made by Lichte's group and others.

The phase distributions of the reconstructed images were successfully used to open up new ways of hitherto inaccessible observations on microscopic states of materials, such as visualizing the magnetic lines of force,[13] equipotential lines,[28] thickness distributions,[14] and inner potentials.[29] Many noteworthy applications are now being developed, such as the observation of magnetic domain structures in ferromagnetic materials,[30–32] dopant distributions in semiconductor devices,[33,34] ferroelectric materials,[35] and vortex behaviors in superconductors.[16,36]

3.2 Fundamental problems with quantum mechanics

The relative phase of an electron wavefunction can now be precisely and directly measured, which has enabled even "thought experiments" to be carried out on the fundamentals of quantum mechanics.

3.2.1 Single-electron build up of interference pattern

An electron interference pattern is formed in such a way that a single electron exists at one time in the "double slit" apparatus. Feynman *et al.*[37] once referred to this type of experiment as "impossible, absolutely impossible to explain in any classical way, and it has

Table I. History of development of bright electron beams.

Year	Electron microscope	Brightness [A/(cm$^2 \cdot$ster)]	Application
1968	100 kV FEEM (Thermionic electrons)	1×10^6	Experimental feasibility of electron holography[7]
1978	80 FEEM	1×10^8	Direct observation of magnetic lines of force[13]
1982	250 FEEM	4×10^8	Conclusive experiments of AB effect[22]
1989	350 FEEM	5×10^9	Dynamic observation of vortices in metal superconductors[15]
2000	1 MV FEEM	2×10^{10}	Observation of unusual behaviors of vortices in high-T_c superconductors[16]

FEEM: field-emission electron microscope in it the heart of quantum mechanics. This experiment has never been done in just this way, since the apparatus would have to be made on an impossibly small scale".

However, these thought experiments have now become feasible with the progress in advanced technologies.[38] Electron microscopy allows small-scale magnification, and individual electrons can be detected with a photon-counting detector (Hamamatsu Photonics PIAS) modified to count individual electrons with almost 100% efficiency of detection. The experiments were actually carried out with a field-emission electron microscope equipped with both an electron biprism and a two-dimensional position-sensitive electron-counting system. As we can observe in Fig. 1, electrons emitted from a field-emission tip are sent to the biprism. The interference pattern is then enlarged by magnifying lenses and is recorded by the electron-counting system. Individual electrons are displayed as bright spots on a TV monitor. When there is a small number of detected electrons, the electron distribution appears to be quite random as can be observed in Figs. 2(a) and 2(b). However, an interference pattern gradually emerges [Fig. 2(c)] when the number of bright spots increases, even when the rate of arriving electrons was as low as 10 electrons/s in the entire field of the view, meaning that at most, only a single electron existed at one time. The accumulated electrons formed the interference pattern as shown in Fig. 2(d), which is formed when the two electron waves of a single electron pass through both sides of the biprism and overlap on the detector plane.

Even a single electron can split into two in the form of a wavefunction on both sides of the biprism. The two partial electron waves then overlap to interfere on the observation plane and form an interference pattern of probability. When detected, however, the overlapped waves are observed as a single electron, never as two. This can be interpreted as the measurement instantly making the extended wavefunctions collapse into a single point.

Our experiment described in Fig. 2 has often been cited in physics textbooks,[39] and was selected and awarded as *The Most Beautiful Experiments* by Physics World,[40,41] which was shared with an electron interference experiment that uses the actual fine multiple slits carried out by Jönsson in 1961.[42]

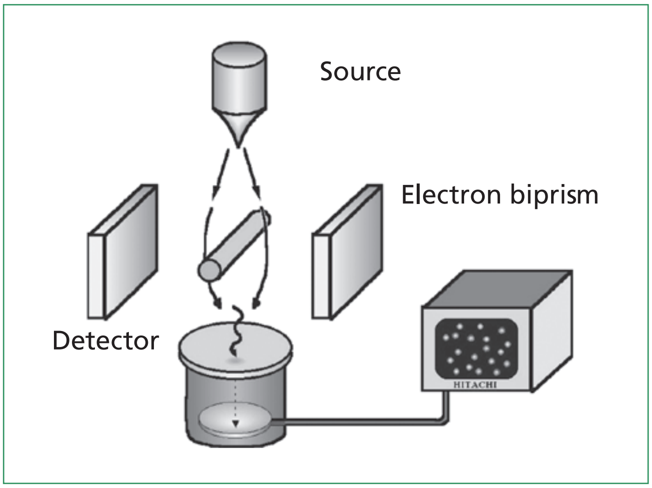

fig. 1. Double-slit experiment for electrons.

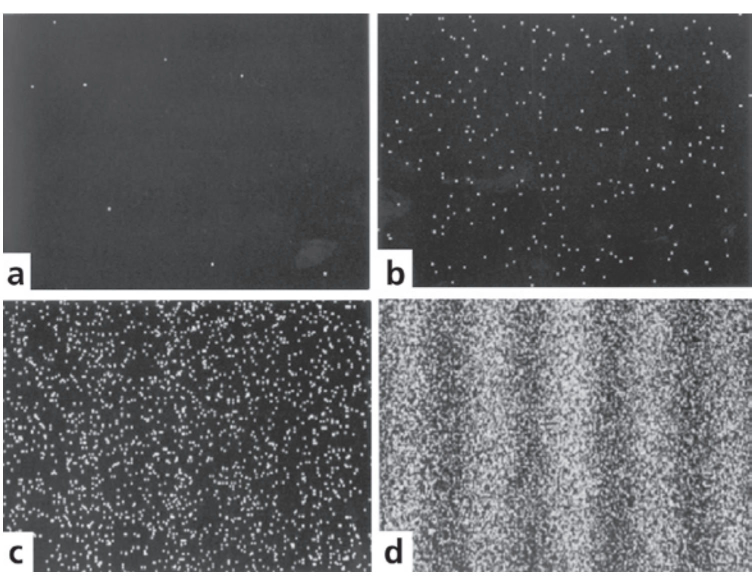

fig. 2. Buildup process of electron interference pattern. Number of electrons: (a) 8; (b) 200; (c) 6,000; (d) 140,000.
The video clip can be seen in http://www.hqrd.hitachi.co.jp/global/fellow_tonomura.cfm

3.2.2 Aharonov–Bohm effect

The inexplicable behavior of electrons is not restricted to the double-slit experiment. The interaction of an electron wave with electromagnetic fields also contradicts our rational, classical concept. For example, electric and magnetic fields are defined as forces exerted on a charged particle. However, the absence of electric and magnetic fields does not necessarily mean the absence of vector potentials. In fact, a beam of charged particles can be physically affected in the form of phase shifts, even when it passes through a region free of magnetic fields outside an infinitely long solenoid and is, therefore, not subjected to any forces. Aharonov and Bohm[43] attributed this effect to vector potentials exciting even in the field-free region outside the solenoid. The reality of vector potentials has been greatly disputed over the past century.[44] When vector potentials were extended to gauge fields particularly in the late 1970s, and regarded as a fundamental physical entity in theories unifying all fundamental forces in nature, the AB effect received much attention as it directly indicated the gauge principle.[45] The existence of the AB effect then began to be questioned.[46] The AB effect has been controversial ever since it was predicted. Until the late 1970s, however, discussions were focused on theoretical interpretations of the AB effect. The experiments carried out in the 1960s were generally believed to demonstrate that the AB effect existed.

Bocchieri and Loinger[47] claimed in 1978 that the AB effect did not exist. They asserted that the AB effect is actually gauge-dependent and is a purely mathematical concoction. According to their analysis, a gauge func-

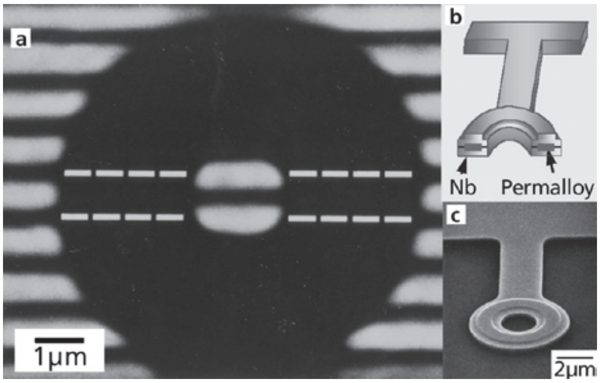

fig. 3. Conclusive experiment of AB effect. (a) Interference pattern; (b) schematic of a sample; (c) scanning electron micrograph of toroidal ferromagnet. Electron waves passing through inside and outside the toroidal magnet are phase-shifted by π by the quantized magnetic flux of $h/(2e)$ though the waves never touch the magnetic fields.

tion can be chosen so that vector potentials completely vanish outside an infinite solenoid: consequently, there is no AB effect.[47,48] They also asserted that the Schrödinger equation can be replaced by a set of nonlinear differential equations called *hydrodynamical equations*, which contain only field strengths $\boldsymbol{E}$ and $\boldsymbol{B}$. There is therefore no room for the AB effect.

They also expressed doubts from experimental viewpoints about the existence of the AB effect:[48] they claimed that the interference experiments must have been affected by leakage fields from solenoids or whiskers.

We carried out a series of experiments to clarify the ambiguities raised in the controversy, and we here introduce our experiment,[22] which is considered to be the most conclusive one.

We used a toroidal ferromagnet instead of a straight solenoid. An infinitely long solenoid is experimentally unable to be attained, but an equally ideal geometry can be achieved by the finite system of a toroidal magnetic field. Furthermore, the toroidal ferromagnet we used was covered with a superconducting niobium layer to completely confine the magnetic field within the toroid.

An electron wave was incident to the tiny toroidal sample fabricated by using the most advanced lithography techniques, and the phase difference between the two waves passing through the hole and around the toroid was measured in the form of an interferogram. If the phase difference is present, it should be given by $e/\hbar$ times the magnetic flux enclosed by the two waves.

Although various magnetic flux values were used in the measurement, the phase difference was always either 0 or π. The conclusions we drew are now obvious. The photograph in Fig. 3 indicates that a relative phase shift of π is produced even when the magnetic fields are confined within the superconductor and shielded from the electron wave. This clearly demonstrates that there is an AB effect. An electron wave is physically affected by the vector potential.

The quantization of the relative phase shift, in this experiment, either 0 or π, proved that the niobium layer surrounding the magnet actually became superconductive. When a superconductor completely surrounds a magnetic flux, the flux is quantized to an integral multiple of quantized flux, $h/2e$. When an odd number of vortices are enclosed inside the superconductor, the relative phase shift becomes π (mod 2π). The phase shift is 0 for an even number of vortices. Therefore, the occurrence of flux quantization can be used to confirm that the niobium layer actually became superconductive, that the superconductor completely surrounded the magnetic flux, and that the Meissner effect prevented any flux from leaking out.

3.3 Imaging microscopic objects using electron phase information

The AB effect can also be used to observe the microscopic distributions of electromagnetic fields within a material. More specifically, the thickness distribution within a specimen of a homogenous material can be observed as thickness contours in the interference micrograph obtained by electron holography.[49] This is because the phase of an electron wave in this case is shifted by the line integral of the inner potential within the specimen along the electron trajectory when the electron wave passes through it. Although phase shifts can, in general, be detected from standard interference patterns "with" a precision of only $2\pi/4$, the precision can be improved to $2\pi/100$ by using a phase-amplification technique peculiar to holography. In fact, this technique has allowed us to the detect changes in thickness due to monatomic steps[14] and carbon nanotubes.[50]

3.3.1 Magnetic lines of force

Phase shift is produced by vector potentials. When the phase distribution is displayed as an interference micrograph, the contour

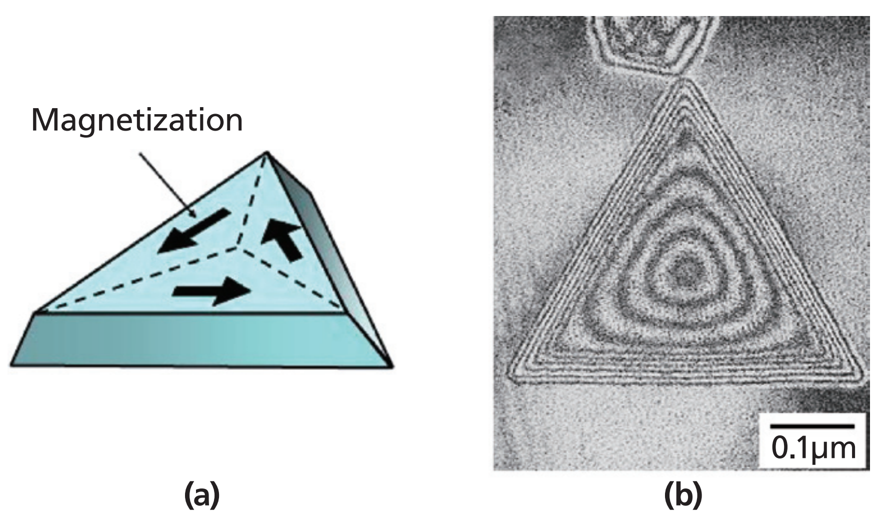

fig. 4. Cobalt fine particle. (a) Schematic diagram; (b) interference micrograph. Only the triangular outline of this particle can be observed by electron microscopy. However, two kinds of contour fringes appear in its interference micrograph: narrow fringes parallel to the edges indicate the thickness contours, and circular fringes in the inner region indicate in-plane magnetic lines of force.

fringes indicate the magnetic lines of force in the magnetic flux units of h/e in the case of pure magnetic fields.

There is an example observation of magnetic lines of force inside a ferromagnetic fine particle in Fig. 4. Narrow fringes parallel to the edges indicate the thickness contours. The circular fringes in the inner region indicate magnetic lines of force, since the thickness is uniform there.

3.3.2 Vortices in superconductors

Vortices inside a superconducting thin film can be visualized as black-and-white spots in a defocused image, or a Lorentz micrograph.[15] When the film is tilted and a magnetic field is applied, thus producing vortices, electrons passing through the vortices in the film are phase-shifted, or deflected, by the vortices' magnetic fields. The vortices can be observed by simply defocusing the electron microscopic image. That is, when the intensity of electrons is observed in an out-of-focus plane, the phase change is transformed into the intensity change and a vortex appears as a pair of bright and dark contrast features.

We can thus observe the dynamics of vortices in real time using the Lorentz microscopy. Observations include the behaviors of vortices at pinning centers and surface steps under various sample temperature and applied magnetic field conditions. In fact, vortices move in interesting ways as if they were living organisms.

There is an interesting example in Fig. 5, where two kinds of vortex images, whose contrasts are reversed, appear in a single field of view. They are actually vortices and antivortices produced in a niobium thin film by applying a magnetic field of 100 G applied to the film and by reversing the polarity of the field. The original vortices would like to exit the film, but cannot immediately do so since they are pinned by defects, whereas the oppositely oriented vortices begin to penetrate into the film from its edges. Where the two streams of vortices and antivortices collide head-on, the heads of the vortex–antivortex of vortex streams annihilate each other. The direct observation of this pair annihilation of vortices can simulate that of particles and antiparticles, since vortices are elementary particles in superconductors in that they cannot be divided any further.

High-T_c superconductors have long been expected to be used in practice, but their low critical currents have impeded the process. Their critical current is low because of their high-temperature operation and their layered structure of materials, both of which enable the vortices to move easily. We developed a 1 MV field-emission electron microscope[18] to investigate the behavior of vortices in high-T_c superconductors. The 1 MV electrons were required to observe the vortices so that the electrons can penetrate a film thicker than the magnetic radius (penetration depth) of vortices in high-T_c superconductors. We observed the internal behavior of vortices inside high-T_c Bi-2212 ($Bi_2Sr_2CaCu_2O_{8+\delta}$) thin films with this microscope.

Columnar defects were produced by irradiating the sample with high-energy heavy ions, which are considered to be optimal pinning traps for vortices in layered structure materials. As shown in the electron micrograph in Fig. 6(a), they are produced in Bi-2212 films as tilted, which can be observed as tiny black lines. When these images are defocused, they are blurred and eventually disappear completely by spreading out. When they are defocused even further, however, vortex images appear, since they are produced by the phase contrast. The resulting Lorentz micrograph of vortices is shown in Fig. 6(b).

The micrograph reveals two different kinds of images, circular and elongated. The elongated images indicated by the arrows in the micrograph are only produced at the locations of the columnar defects and correspond to vortices trapped along the tilted columns. We confirmed the validity of this interpretation in the simulation. The circular images are produced in regions without defects, and therefore correspond to vortices perpendicularly penetrating the film. This has enabled us to use the vortex images to investigate whether vortices are trapped or not under various conditions.[51)]

3.3.3 Unusual behaviors of vortices in high-T_c superconductors

Vortices usually form a closely packed triangular lattice.[52] This occurs even in anisotropic high-T_c superconductors, as long as the magnetic field is directed along the anisotropy c-axis. When the magnetic field is steeply tilted away from the c-axis, however, Bitter images reveal that the vortices no longer form a triangular lattice. Instead, they form arrays of linear chains along the direction of the tilted field as observed in YBCO ($YBaCu_3O_{7-\delta}$),[53] or alternating domains of chains and triangular lattices as in Bi-2212.[54,55] While the chain

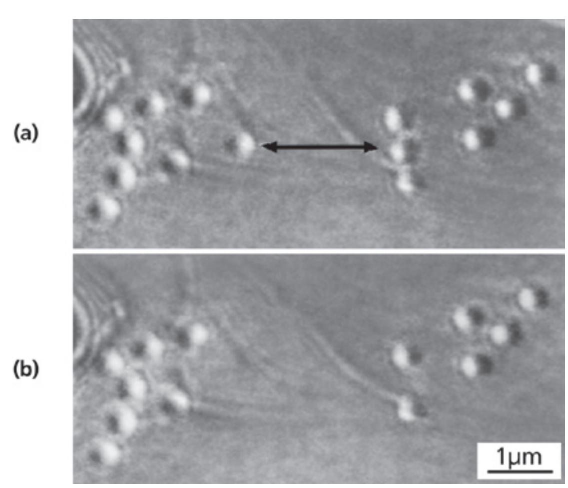

fig. 5. Annihilation of vortices and antivortices in thin film of niobium. (a) Before annihilation; (b) after annihilation. When the magnetic field applied to the film is suddenly reversed, some vortices remain at defects, whereas others begin to leave them. Antivortices begin to move in from the edges of the film. Where streams of vortices and antivortices collide head-on, the vortex–antivortex pairs of the heads of the two streams annihilate each other.

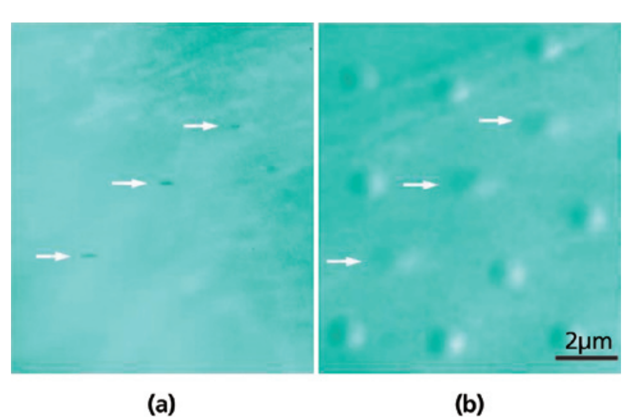

fig. 6. Comparison of columnar-defect image and vortices in Bi-2212 thin film. (a) Electron micrograph; (b) Lorentz micrograph. Some vortices are trapped at columnar defects and others are untrapped. The images of untrapped vortex lines perpendicular to the film plane are circular spots having bright and dark regions. Vortex images located at the positions of columnar defects are elongated spots with lower contrast indicated by the arrows, since these vortex lines are trapped at columnar defects tilted at 70°.

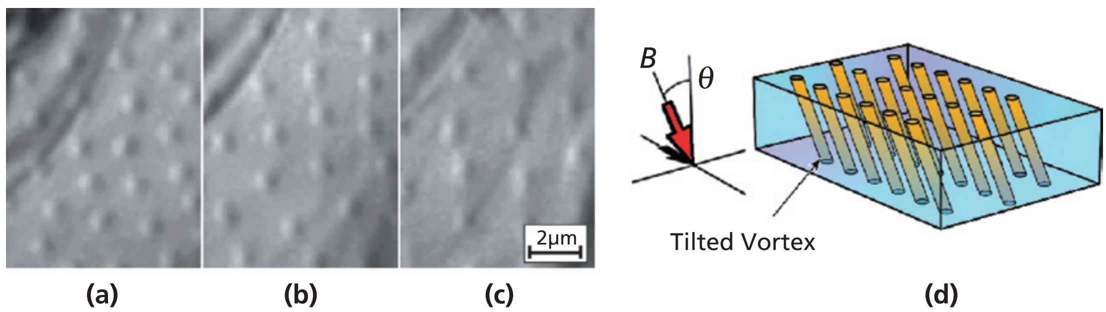

fig. 7. Lorentz micrographs of vortices in YBCO film sample at tilted magnetic fields (T = 30K; B_p = 3G). (a) θ = 75°, (b) θ = 82°, (c) θ = 83°. (d) Schematic of tilted vortex lines. When the tilt angle θ becomes larger than 75°, the vortex images begin to elongate and, at the same time, form arrays of linear chains.

state in YBCO can be explained by the tilting of vortex lines within the framework of the anisotropic London theory, the chain-lattice state in Bi-2212 has long been an object of discussion. For example, Grigorieva and Steeds[55)] concluded from both Bitter observations that the chain vortices and lattice vortices are both tilted, but in different directions. On the other hand, Huse[56)] suggested two sets of vortices, one set running parallel to the layers and the other set running normal to the layers. However, this model was not able to explain why the two perpendicular vortices cross each other to form stable chains, since no interaction takes place between the two perpendicular magnetic fields.

In 1999, Koshelev[57)] proposed a solution for the chain-lattice state; Josephson vortices penetrate between the layer planes and the pancake vortices that perpendicularly intersect the Josephson vortices form chains; the rest of the vortices form triangular lattices. However, Koshelev considered the second-order approximation and determined that there was energy reduction in this vortex arrangement by assuming that a vertical vortex line winds slightly in opposite directions just above and below the crossing Josephson vortex as a result of the interaction with the Josephson vortex; the circulating supercurrent of the Josephson vortex exerts Lorentz forces on the vertical vortex line.

No direct evidence for such mechanisms, however, was found through experiments because of the lack of methods of directly observing the arrangements of vortex lines *inside* superconductors. Lorentz microscopy with our 1MV electron microscope was used to determine whether the vortex lines in the chain states inside high-T_c superconductors were tilted or not.

We found that vortex lines in YBCO are tilted together in the direction of the applied magnetic field, as is evident from the Lorentz

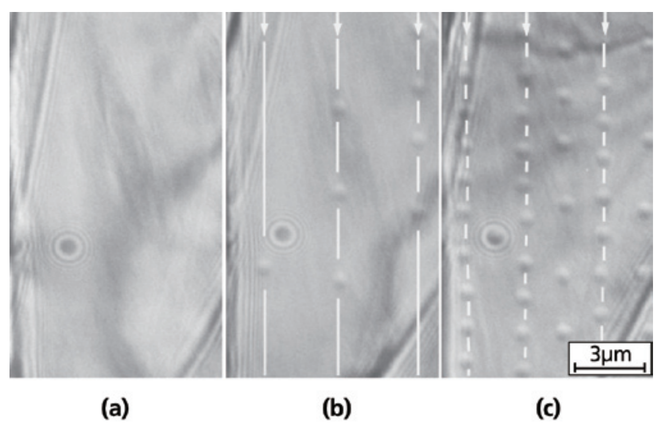

fig. 8. Series of Lorentz micrographs of vortices in field-cooled Bi-2212 film sample when magnetic field B_p perpendicular to layer plane begins to be applied and increases at fixed in-plane magnetic field of 50G at T = 50K. (a) B_p = 0; (b) B_p = 0.2G; (c) B_p = 1G.

micrographs in Fig. 7, where the vortex images became more elongated and formed linear chains together as the tilting angle of the magnetic field increased. In the case of Bi-2212, our observations by Lorentz microscopy revealed that neither chain vortices nor lattice vortices tilted, but both stood perpendicular to the layer plane.[58)] In our present experiment, we were not able to detect the slight windings of the pancake vortex lines Koshelev predicted. If vortex lines were tilted at an angle comparable to that of the applied magnetic field, the vortex images in Fig. 8 should have been elongated.

Our finding that both chain vortices and lattice vortices in Bi-2212 stand straight almost perpendicular to the film plane and do not tilt is clear evidence of the Koshelev mechanism. Although the clearest evidence for this model would of course be given if Josephson vortices were observed along chain vortices. However, the magnetic field of a Josephson vortex extends widely between the layers, therefore making it difficult to detect with our method.

When a magnetic field is applied parallel to the layer plane, no vertical vortices are produced; therefore, no vortex images can be observed in Fig. 8(a). Even though Josephson vortices parallel to the layer plane should exist, these vortices cannot be observed by Lorentz microscopy because of the wide distribution of the vortex magnetic field. When the vertical magnetic field B_p increases, vertical vortices begin to appear along straight lines indicated by the white arrows in Fig. 8(b), which are considered to be determined by Josephson vortices. Since vortices are arranged along straight lines, we could find no other reason for the production of chain vortices other than assuming that vertical vortices crossing Josephson vortices form chains. Above B_p = 1G, vertical vortices also appear between chain vortices, as shown in (c).

The vortices do not form a closely packed triangular lattice, but they are located along straight lines [Figs. 8(b) and 8(c)]. The reason they appear along straight lines is that perpendicular vortices tend to line up densely along the Josephson vortices.

4. Conclusions

Some experiments that were once regarded as "thought experiments" can now be carried out because of recent developments in advanced technologies such as coherent electron beams, highly sensitive electron detectors, and photolithography. In addition, the wave nature of electrons can now be utilized to observe microscopic objects that were previously unobservable. Examples are the quantitative observation of both the microscopic distribution of magnetic lines of force in h/e units and the dynamics of quantized vortices in superconductors. This measurement and observation technique is expected to play an important role in future research and development in nanoscience and related technology.

JSAP

1) D. Gabor: Proc. R. Soc. London, Ser. A **197** (1949) 454.
2) H. Boersch: Naturwissenschaften **28** (1940) 711 [in German].
3) M. E. Haine and T. Mulvey: J. Opt. Soc. Am. **42** (1952) 763.
4) T. Hibi: J. Electron Microsc. **4** (1956) 10.
5) E. N. Leith and J. Upatnieks: J. Opt. Soc. Am. **52** (1962) 1123.
6) J. B. DeVelis, G. B. Parrent, and B. J. Thompson: J. Opt. Soc. Am. **56** (1966) 423.
7) A. Tonomura, A. Fukuhara, H. Watanabe, and T. Komoda: Jpn. J. Appl. Phys. **7** (1968) 295.
8) G. Möllenstedt and H. Wahl: Naturwissenschaften **55** (1968) 340 [in German].
9) E. W. Müller: Z. Phys. **106** (1937) 541 [in German].
10) A. V. Crewe, D. N. Eggenbeerger, D. N. Wall, and L. N. Welter: Rev. Sci. Instrum. **39** (1968) 576.
11) A. V. Crewe, J. Wall, and J. Langmore: Science **168** (1970) 1338.
12) A. Tonomura, T. Matsuda, J. Endo, H. Todokoro, and T. Komoda: J. Electron Microsc. **28** (1979) 1.
13) A. Tonomura, T. Matsuda, J. Endo, T. Arii, and K. Mihama: Phys. Rev. Lett. **44** (1980) 1430.
14) A. Tonomura, T. Matsuda, T. Kawasaki, J. Endo, and N. Osakabe: Phys. Rev. Lett. **54** (1985) 60.
15) K. Harada, T. Matsuda, J. Bonevich, M. Igarashi, S. Kondo, G. Pozzi, U. Kawabe, and A. Tonomura: Nature **360** (1992) 51.
16) A. Tonomura, H. Kasai, O. Kamimura, T. Matsuda, K. Harada, Y. Nakayama, J. Shimoyama, K. Kishio, T. Hanaguri, K. Kitazawa, M. Sasase, and S. Okayasu: Nature **412** (2001) 620.
17) T. Kawasaki, T. Matsuda, J. Endo, and A. Tonomura: Jpn. J. Appl. Phys. **29** (1990) L508.
18) T. Kawasaki, T. Yoshida, T. Matsuda, N. Osakabe, A. Tonomura, I. Matsui, and K. Kitazawa: Appl. Phys. Lett. **76** (2000) 1342.
19) T. Akashi, K. Harada, T. Matsuda, H. Kasai, A. Tonomura, T. Furutsu, N. Moriya, T. Yoshida, T. Kawasaki, K. Kitazawa, and H. Koinuma: Appl. Phys. Lett. **81** (2002) 1922.
20) A. Tonomura, T. Matsuda, R. Suzuki, A. Fukuhara, N. Osakabe, H. Umezaki, J. Endo, K. Shinagawa, Y. Sugita, and H. Fujiwara: Phys. Rev. Lett. **48** (1982) 1443.
21) A. Tonomura, H. Umezaki, T. Matsuda, N. Osakabe, J. Endo, and Y. Sugita: Phys. Rev. Lett. **51** (1983) 331.
22) A. Tonomura, N. Osakabe, T. Matsuda, T. Kawasaki, J. Endo, S. Yano, and H. Yamada: Phys. Rev. Lett. **56** (1986) 792.
23) J. Munch: Optik **43** (1975) 79.
24) A. Tonomura, T. Matsuda, and J. Endo: Jpn. J. Appl. Phys. **18** (1979) 9.
25) A. Tonomura, T. Matsuda, and J. Endo: Jpn. J. Appl. Phys. **18** (1979) 1373.
26) H. Lichte: Optik **70** (1985) 176.
27) A. Orchowski, W. D. Rau, and H. Lichte: Phys. Rev. Lett. **74** (1995) 399.
28) S. Frabboni, G. Matteucci, and G. Pozzi: Phys. Rev. Lett. **55** (1985) 2196.
29) M. Gajdardziska-Josifovska, M. R. McCartney, W. J. de Ruijter, D. J. Smith, J. K. Weiss, and J. M. Zuo: Ultramicroscopy **50** (1993) 285.
30) R. E. Dunin-Borkowski, M. R. McCartney, B. Kardynal, M. R. Scheinfein, D. J. Smith, and S. S. P. Parkin: J. Appl. Phys. **90** (2001) 2899.
31) D. Shindo, Y. G. Park, and Y. Yoshizawa: J. Magn. Magn. Mater. **238** (2002) 101.
32) Y. Zhu, V. V. Volkov, and M. De Graef: J. Electron Microsc. **50** (2001) 447.
33) W. D. Rau, P. Schwander, F. H. Baumann, W. Höppner, and A. Ourmazd: Phys. Rev. Lett. **82** (1999) 2614.
34) Z. Wang, T. Kato, N. Shibata, T. Hirayama, N. Kato, K. Sasaki, and H. Saka: Appl. Phys. Lett. **81** (2002) 478.
35) H. Lichte, M. Reibold, K. Brand, and M. Lehmann: Ultramicroscopy **93** (2002) 199.
36) T. Matsuda, S. Hasegawa, M. Igarashi, T. Kobayashi, M. Naito, H. Kajiyama, J. Endo, N. Osakabe, and A. Tonomura: Phys. Rev. Lett. **62** (1989) 2519.
37) R. P. Feynman, R. B. Leighton, and M. Sands: *The Feynman Lectures on Physics* (Addison-Wesley, Reading, MA, 1965) Vol. III, p. 1.1.
38) A. Tonomura, J. Endo, T. Matsuda, T. Kawasaki, and H. Ezawa: Am. J. Phys. **57** (1989) 117.
39) For example, P. A. Tipler: *Physics* (Freeman Worth, New York, 1999) 4th ed., p. 509.
40) R. P. Crease: Phys. World **15** (2002) No. 9, 19.
41) R. P. Crease: *The Prism and the Pendulum: The Ten Most Beautiful Experiments in Science* (Random House, New York, 2003) p. 190.
42) C. Jönsson: Z. Phys. **161** (1961) 454 [in German].
43) Y. Aharonov and D. Bohm: Phys. Rev. **115** (1959) 485.
44) C. N. Yang: in *Quantum Coherence and Decoherence*, ed. K. Fujikawa and Y. A. Ono (Elsevier, Amsterdam, 1996) p. 307.
45) T. T. Wu and C. N. Yang: Phys. Rev. D **12** (1975) 3845.
46) M. Peshkin and A. Tonomura: *Lecture Notes in Physics* (Springer, Heidelberg, 1989) Vol. 340.
47) P. Bocchieri and A. Loinger: Nuovo Cimento A **47** (1978) 475.
48) P. Bocchieri, A. Loinger, and G. Siragusa: Nuovo Cimento A **51** (1979) 1.
49) A. Tonomura: *Electron Holography* (Springer, Heidelberg, 1999) 2nd ed.
50) Q. Ru, G. Lai, K. Aoyama, J. Endo, and A. Tonomura: Ultramicroscopy **55** (1994) 209.
51) A. Tonomura, H. Kasai, O. Kamimura, T. Matsuda, K. Harada, Y. Nakayama, J. Shimoyama, K. Kishio, T. Hanaguri, K. Kitazawa, M. Sasase, and S. Okayasu: Physica C **369** (2002) 68.
52) U. Essmann and H. Träuble: Phys. Lett. A **24** (1967) 526.
53) P. L. Gammel, D. J. Bishop, J. P. Rice, and D. M. Ginsberg: Phys. Rev. Lett. **68** (1992) 3343.
54) C. A. Bolle, P. L. Gammel, D. G. Grier, C. A. Murray, D. J. Bishop, D. B. Mitzi, and A. Kapitulnik: Phys. Rev. Lett. **66** (1991) 112.
55) I. V. Grigorieva and J. W. Steeds: Phys. Rev. B **51** (1995) 3765.
56) D. A. Huse: Phys. Rev. B **46** (1992) 8621.
57) A. E. Koshelev: Phys. Rev. Lett. **83** (1999) 187.
58) A. Tonomura, H. Kasai, O. Kamimura, T. Matsuda, K. Harada, T. Yoshida, T. Akashi, J. Shimoyama, K. Kishio, T. Hanaguri, K. Kitazawa, T. Matsui, S. Tajima, N. Koshizuka, P. L. Gammel, D. Bishop, M. Sasase, and S. Okayasu: Phys. Rev. Lett. **88** (2002) 237001.

Akira Tonomura is a fellow of Hitachi, Ltd., a group director of RIKEN, and a principal investigator of Okinawa Institute of Science and Technology. He graduated from the University of Tokyo, Department of Physics, in 1965 and joined Hitachi, Ltd. Since then, he has been engaged in experimental researches on electron physics using electron microscopes. From 1973 he stayed for one year at Tübingen University to research on electron interferometry. He served concurrently as the director of the national "Electron Wavefront Project" (ERATO) from 1989 to 94. He was awarded the Nishina Memorial Prize in 1982, the Japan Academy Prize and Imperial Prize in 1991, and the Benjamin Franklin Medal in physics in 1999. In 2000, he was elected as a foreign associate of the National Academy of Sciences in the United States. Since 2005, he has been also elected as a member of Science Council of Japan. He is now a member of the Japan Academy.

He is recognized for his pioneering work in the new field of electron holography which was made possible by the development of "coherent" field-emission electron beams. This method is used for the direct observation of both microscopic electromagnetic fields and magnetic vortices in superconductors, and the verification of fundamental phenomena in quantum mechanics such as Aharonov–Bohm effect and single-electron build-up of an interference pattern.